

SUPPLEMENTARY INFORMATION

I. Additional Experimental Results and Details.

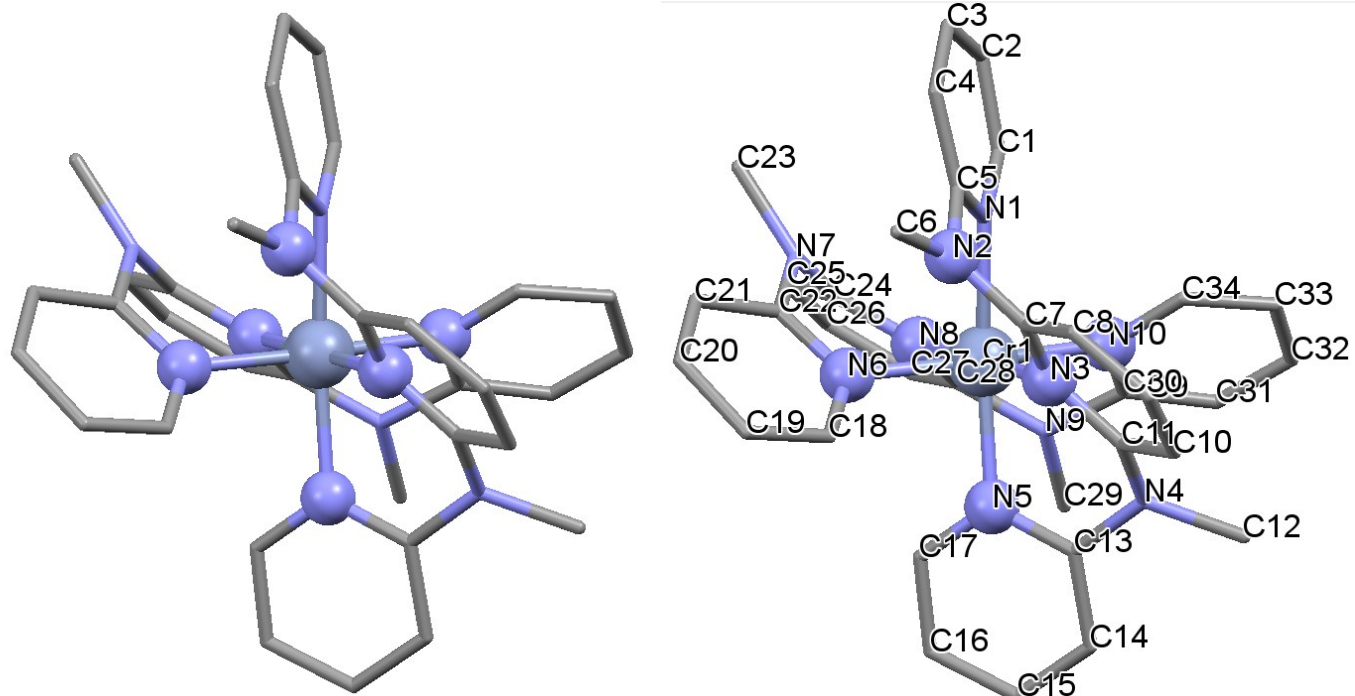
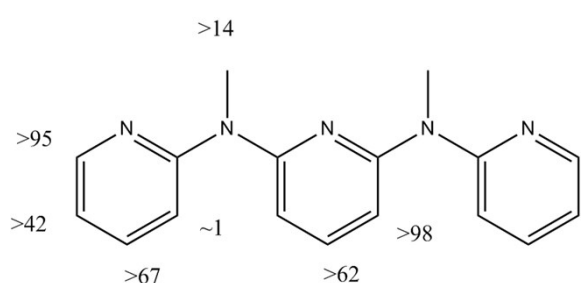
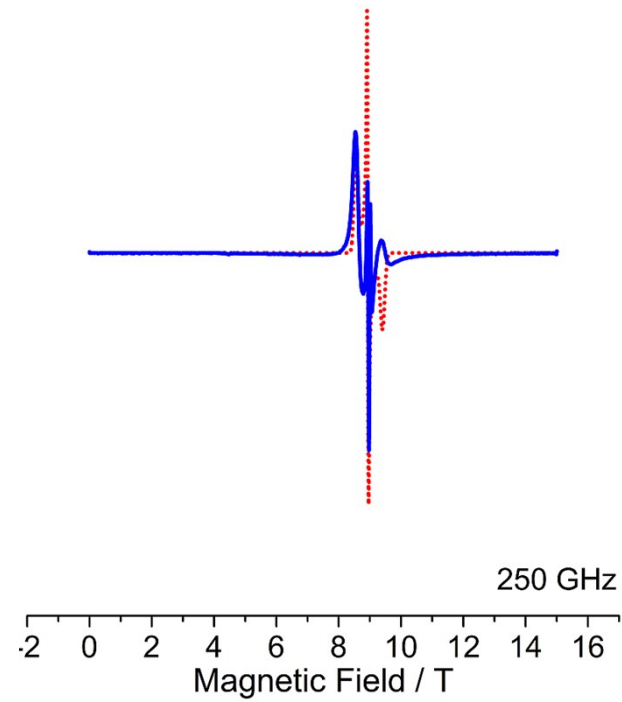
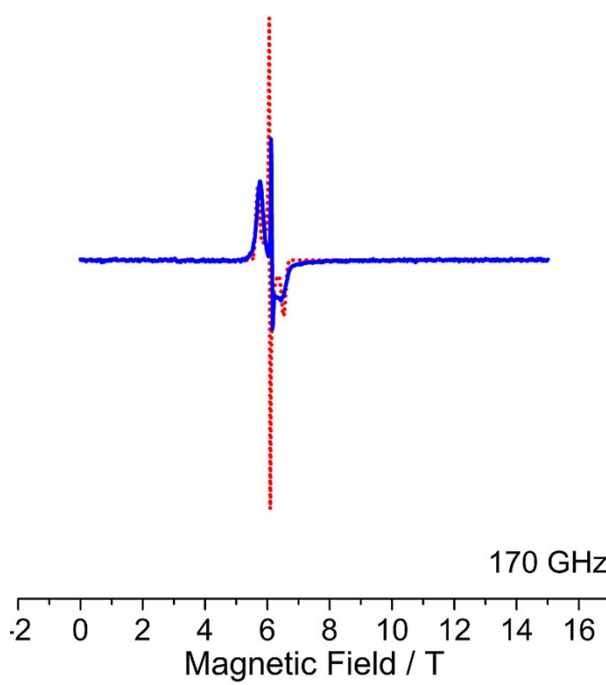
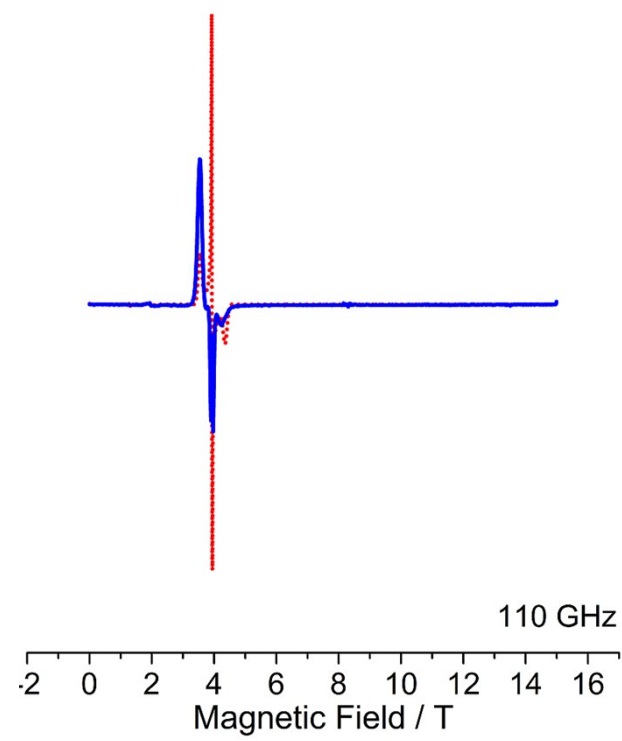
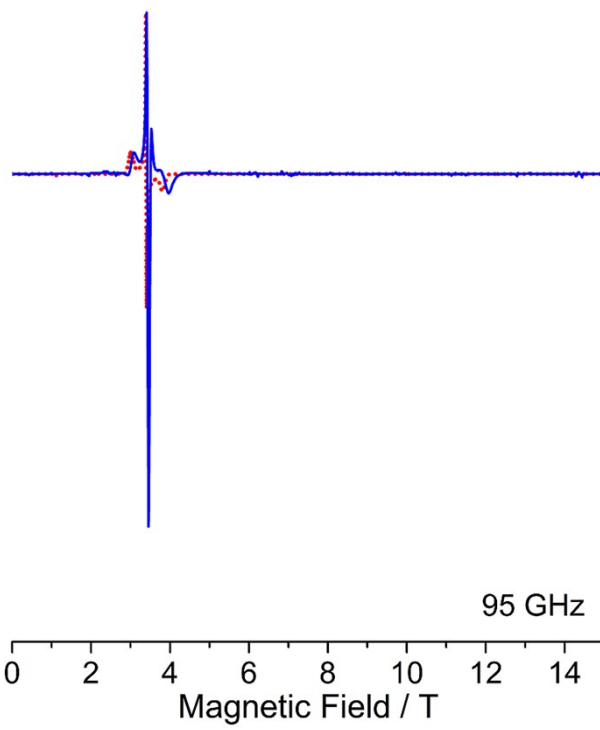


Figure S1. Molecular structure of **1H** with the central chromium and coordinating nitrogen atoms in ball-and-stick representation and carbon atoms in capped-stick representation. Hydrogens have been omitted. The image on the right includes the atomic labelling.<sup>1</sup>



[D<sub>9</sub>]-ddpd

Figure S2. [D<sub>9</sub>]-ddpd ligand with deuteration percentages. Adapted from Ref. 1.



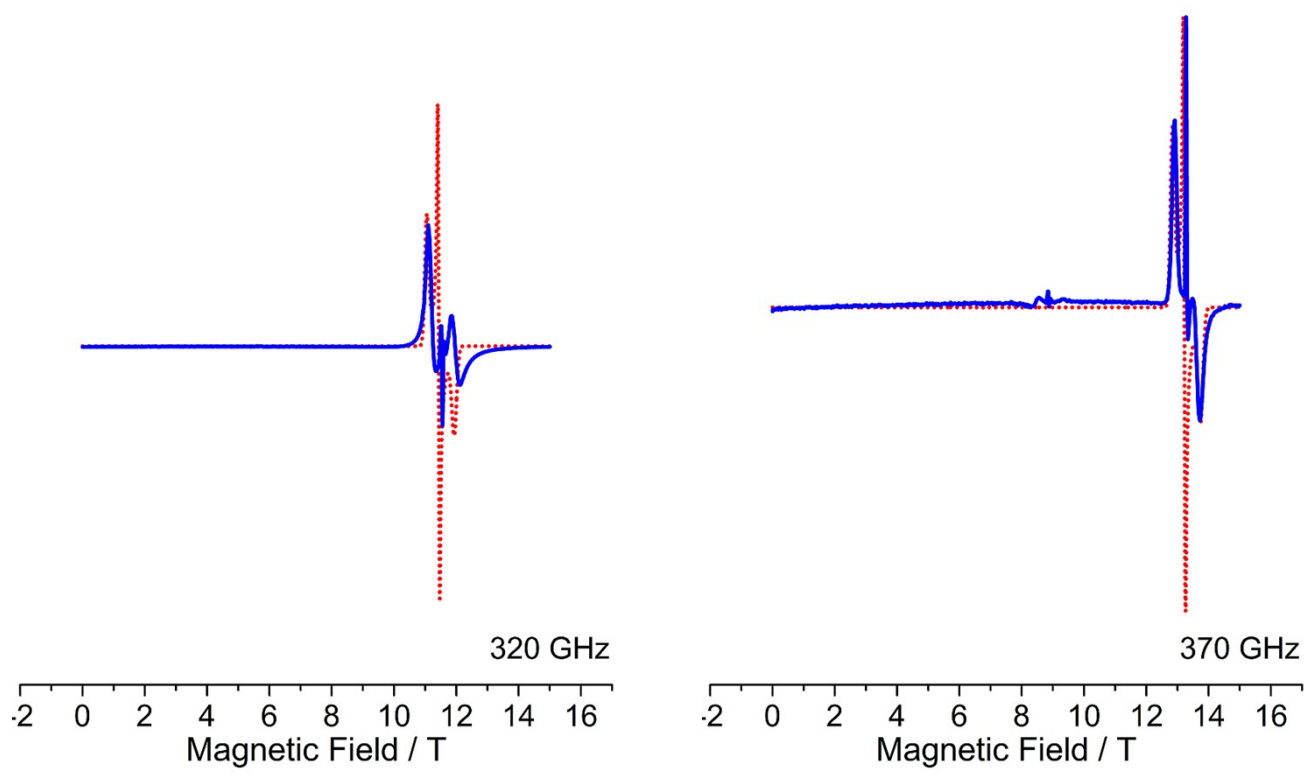


Figure S3. Individual HFEPR spectra and fits corresponding to the overview in Fig. 2 of the main text

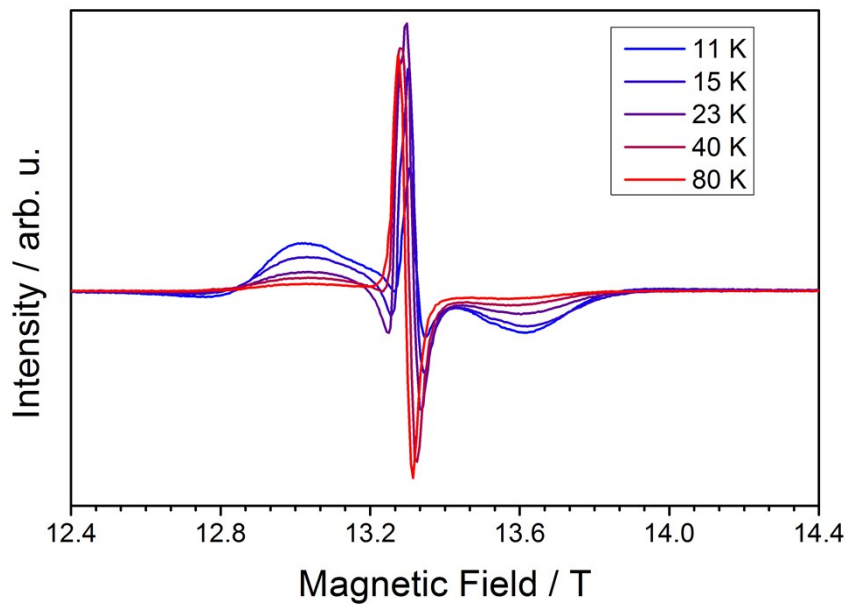


Figure S4 HFEPR spectra recorded on pressed powder pellets of **1H** at 370 GHz and different temperatures as indicated

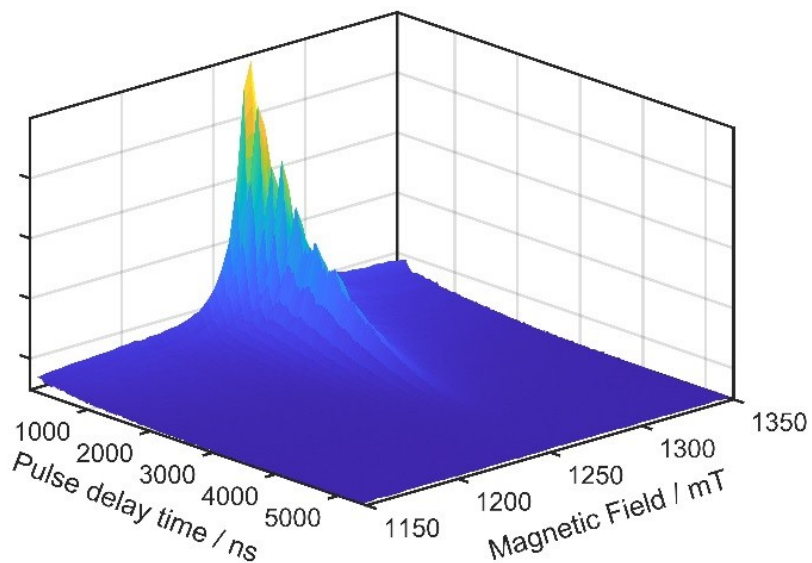


Figure S5 Echo intensity of **1H** in H<sub>2</sub>O:glycerol (1:1 v/v) at 7 K as function of 2τ delay time and magnetic field.

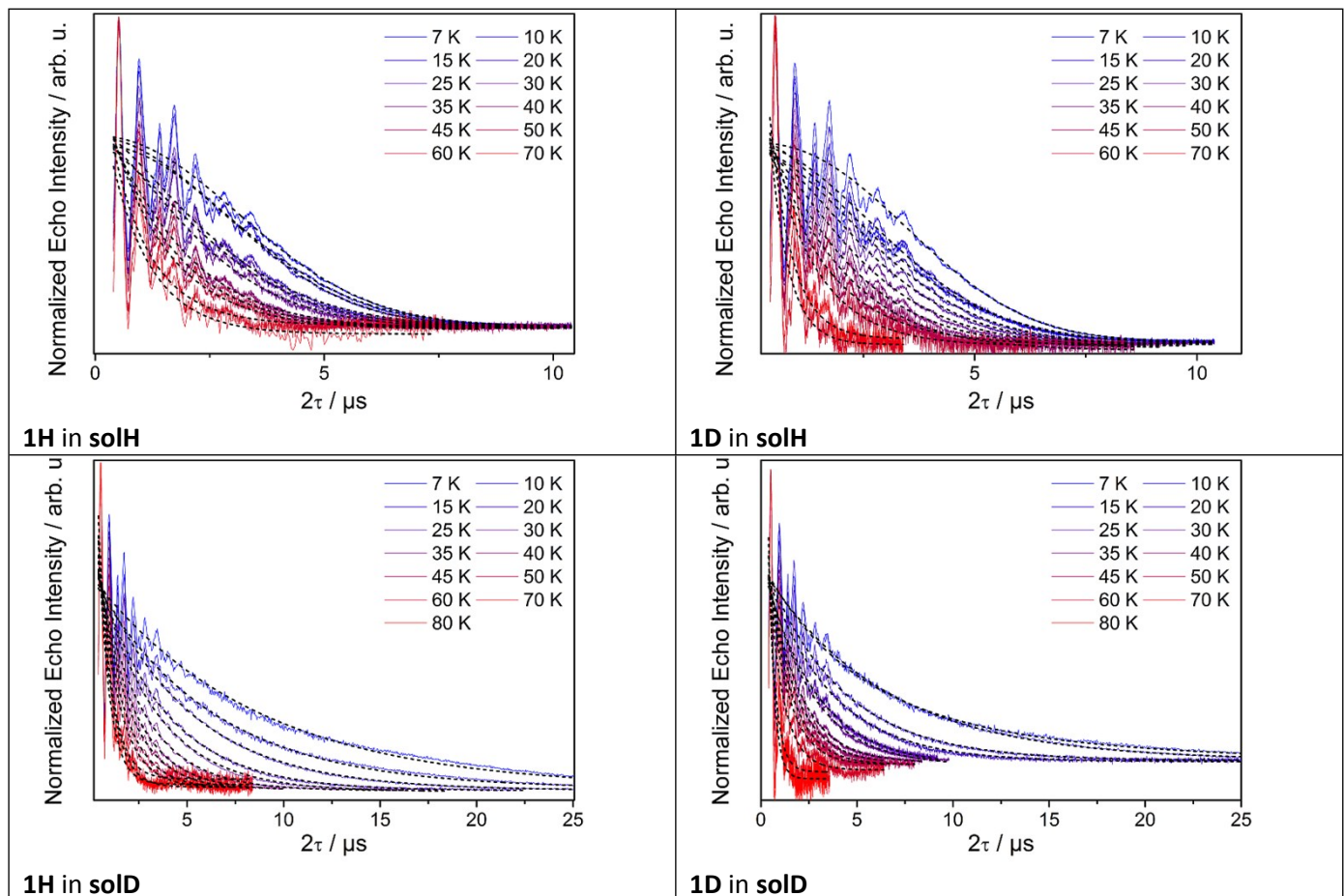
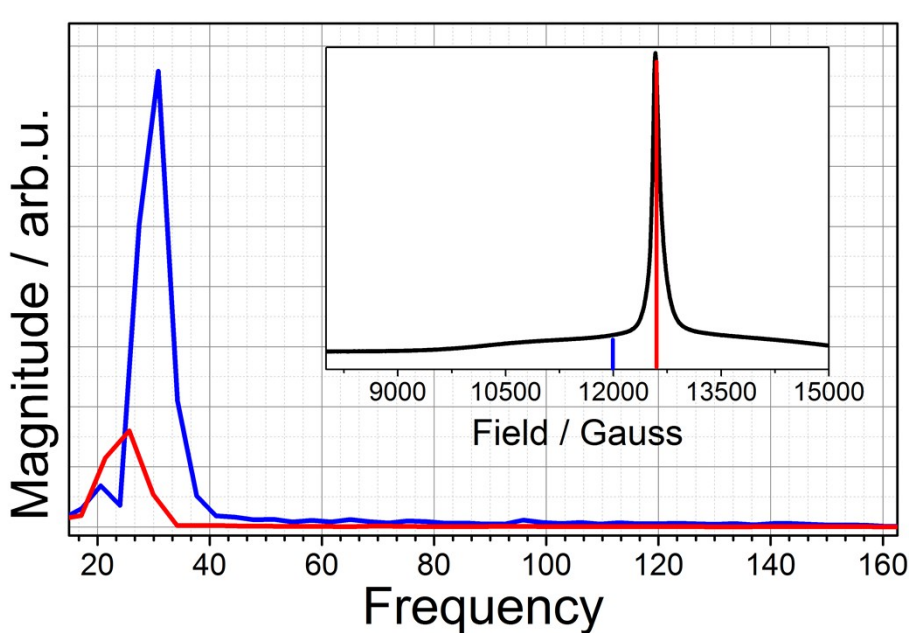
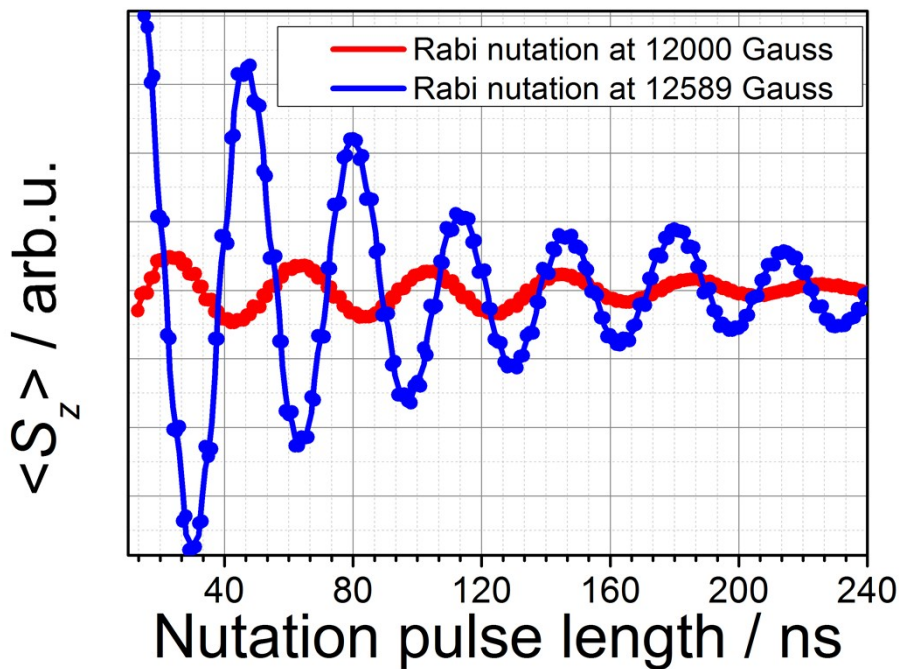


Figure S6. Hahn echo decay curves with fits at various temperatures for the different sample/solvent combinations.



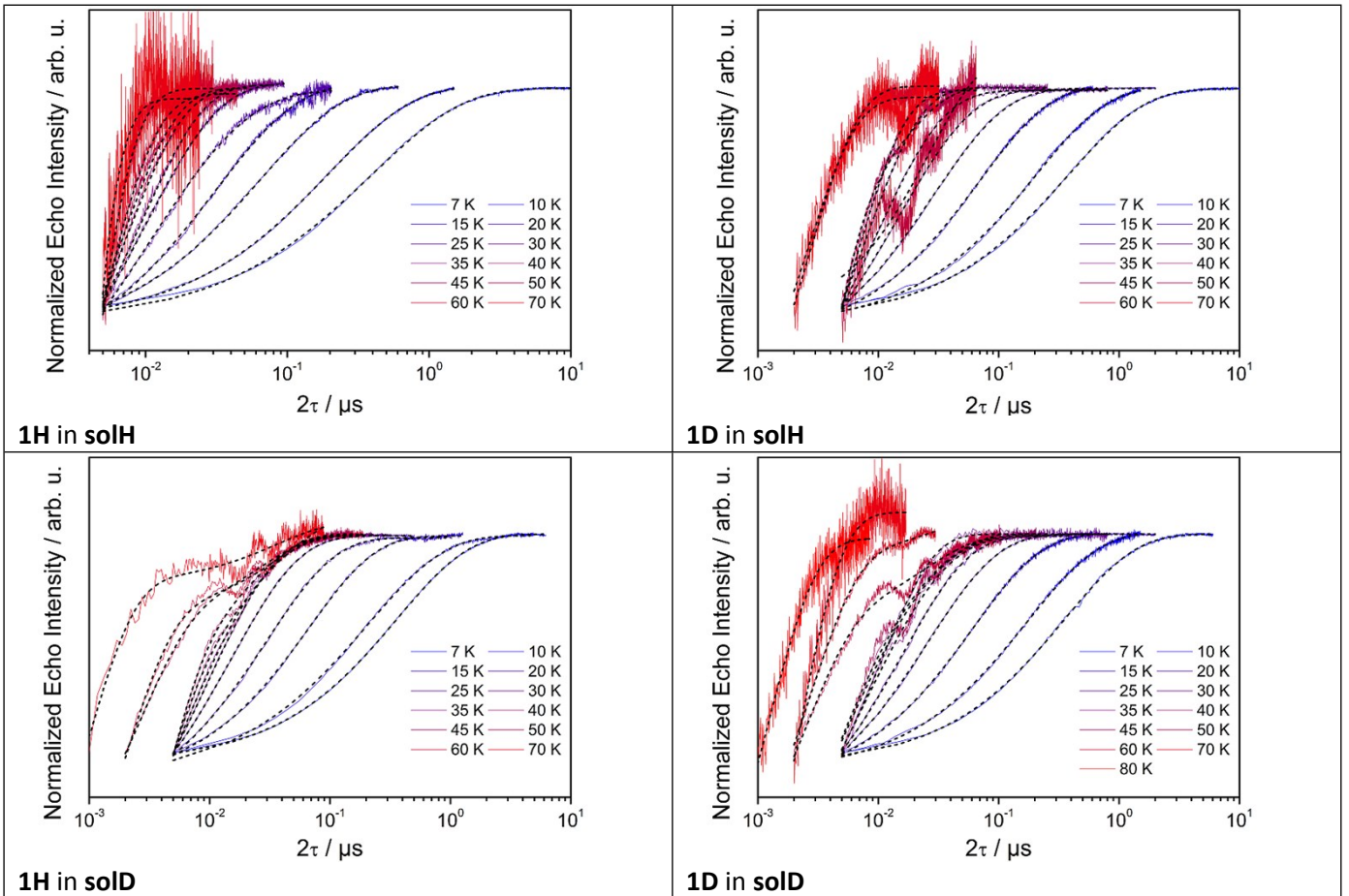


Figure S9. Inversion recovery curves with fits at various temperatures for the different sample/solvent combinations.

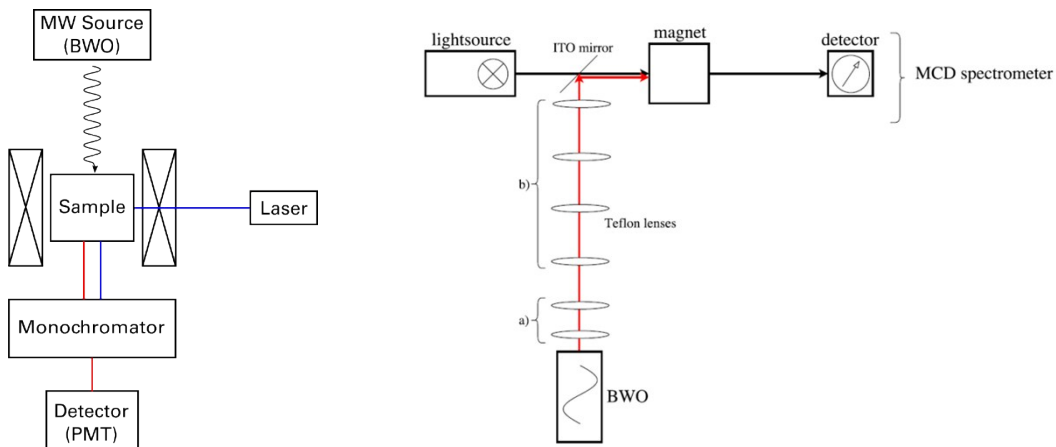


Figure S10 Setup for recording fluorescence-detected EPR.

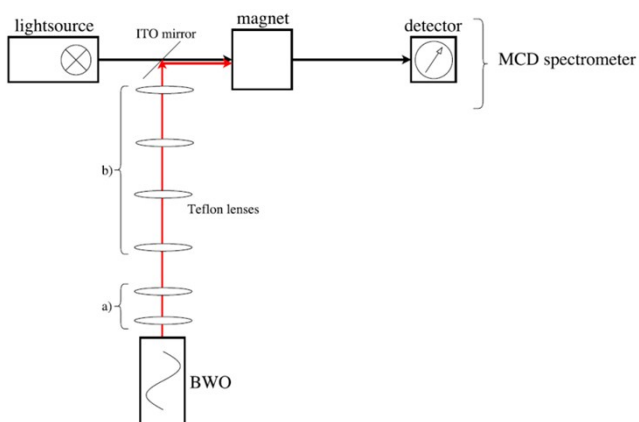


Figure S11 Setup for recording MCD-detected EPR.

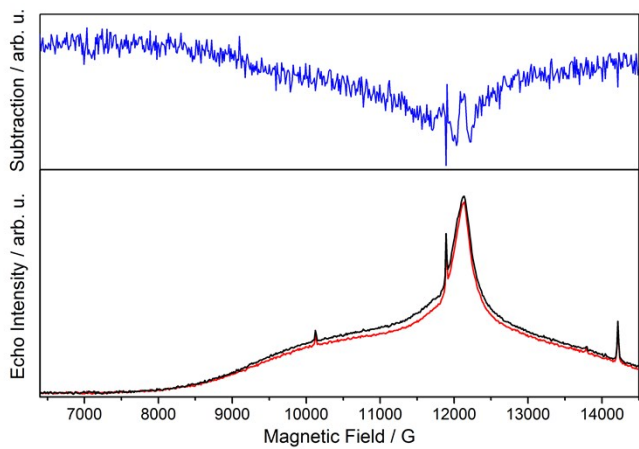


Figure S12 (bottom panel) Echo detected spectra of recorded on 5 mM frozen solutions of **1H** in  $\text{H}_2\text{O}$ :glycerol directly after laser illumination (red) and without irradiation (black) at 33.755 GHz and 7 K. The laser wavelength was 435 nm, the pulse energy 1.2 mJ and the pulse length was 10 ns. The pulse sequence was Laser-2ns- $\pi/2$ - $\tau_{\text{fix}}$ - $\pi$ - $\tau_{\text{fix}}$ -echo. (top panel) Difference between illuminated and non-illuminated spectra.

Table S 1 Fitting parameters (Eq. 4) of the echo decays of **1H** and **1D** 1mM in **solH** and **solD** at 1258 mT, 35 GHz and different temperatures.

T / K	<b>1D/solD</b>		<b>1H/solD</b>		<b>1D/solH</b>		<b>1H/solH</b>	
	$T_m$ / $\mu\text{s}$	$k$	$T_m$ / $\mu\text{s}$	$k$	$T_m$ / $\mu\text{s}$	$k$	$T_m$ / $\mu\text{s}$	$k$
7	$6.629 \pm 0.005$	$8.4 \pm 0.1$	$4.47 \pm 0.03$	$2.29 \pm 0.06$	$4.24 \pm 0.04$	$2.09 \pm 0.05$		
10	$6.266 \pm 0.005$	$6.08 \pm 0.07$	$3.58 \pm 0.04$	$1.58 \pm 0.04$	$3.99 \pm 0.04$	$1.91 \pm 0.05$		
15	$3.92 \pm 0.04$	$4.73 \pm 0.07$	$3.85 \pm 0.04$	$1.89 \pm 0.05$	$3.97 \pm 0.03$	$2.11 \pm 0.06$		
20	$3.34 \pm 0.07$	$3.49 \pm 0.07$	$3.45 \pm 0.04$	$1.71 \pm 0.05$	$3.00 \pm 0.04$	$1.44 \pm 0.05$		
25	$2.73 \pm 0.05$	$2.98 \pm 0.07$	$3.10 \pm 0.04$	$1.59 \pm 0.05$	$3.04 \pm 0.04$	$1.56 \pm 0.05$		
30	$2.40 \pm 0.04$	$2.33 \pm 0.06$	$2.65 \pm 0.05$	$1.41 \pm 0.05$	$2.65 \pm 0.04$	$1.46 \pm 0.05$		
35	$1.65 \pm 0.04$	$1.86 \pm 0.06$	$2.20 \pm 0.06$	$1.24 \pm 0.06$	$1.70 \pm 0.06$	$1.06 \pm 0.05$		
40	$1.44 \pm 0.03$	$1.60 \pm 0.05$	$1.93 \pm 0.07$	$1.18 \pm 0.06$	$1.88 \pm 0.06$	$1.18 \pm 0.05$		
45	$1.21 \pm 0.03$	$1.28 \pm 0.04$	$1.30 \pm 0.02$		$1.45 \pm 0.03$			
50	$1.05 \pm 0.03$	$1.07 \pm 0.03$	$1.12 \pm 0.03$		$1.31 \pm 0.03$			
60	$0.77 \pm 0.03$	$0.66 \pm 0.02$	$0.56 \pm 0.03$		$1.00 \pm 0.02$			
70	$0.37 \pm 0.02$	$0.70 \pm 0.02$	$0.44 \pm 0.03$		$0.9 \pm 0.1$			
80	$0.29 \pm 0.02$	$0.57 \pm 0.02$						

Table S 2 Fitting parameters of the inversion recovery experiments of **1H** and **1D** 1mM in **solH** and **solD** at 1258 mT, 35 GHz and different temperatures.

T / K	<b>1D/solD</b>		<b>1H/solD</b>		<b>1D/solH</b>		<b>1H/solH</b>	
	$T_1$ / ms	$k$						
7	$0.353 \pm 0.002$	$0.735 \pm 0.003$	$0.363 \pm 0.002$	$0.730 \pm 0.002$	$0.363 \pm 0.002$	$0.730 \pm 0.002$	$0.395 \pm 0.002$	$0.676 \pm 0.002$
10	$0.173 \pm 0.001$	$0.728 \pm 0.004$	$0.204 \pm 0.002$	$0.677 \pm 0.005$	$0.204 \pm 0.002$	$0.677 \pm 0.005$	$0.1969 \pm 0.0004$	$0.731 \pm 0.002$
15	$0.0617 \pm 0.0004$	$0.766 \pm 0.004$	$0.0671 \pm 0.0008$	$0.784 \pm 0.007$	$0.0671 \pm 0.0008$	$0.784 \pm 0.007$	$0.0655 \pm 0.0003$	$0.754 \pm 0.003$
20	$0.0255 \pm 0.0004$	$0.736 \pm 0.006$	$0.0298 \pm 0.0005$	$0.763 \pm 0.008$	$0.0298 \pm 0.0005$	$0.763 \pm 0.008$	$0.0309 \pm 0.0004$	$0.742 \pm 0.008$
25	$0.0159 \pm 0.0003$	$0.790 \pm 0.008$	$0.0150 \pm 0.0002$	$0.758 \pm 0.004$	$0.0150 \pm 0.0001$	$0.758 \pm 0.004$	$0.0105 \pm 0.0005$	$0.61 \pm 0.02$
30	$0.0102 \pm 0.0003$	$0.99 \pm 0.02$	$0.0098 \pm 0.0001$	$0.771 \pm 0.004$	$0.0098 \pm 0.0001$	$0.771 \pm 0.004$	$0.0097 \pm 0.0001$	$0.812 \pm 0.008$
35	$0.0070 \pm 0.0005$	$0.60 \pm 0.02$	$0.0045 \pm 0.0002$		$0.0045 \pm 0.0002$		$0.0095 \pm 0.0001$	
40	$0.0037 \pm 0.0007$	$0.49 \pm 0.03$	$0.0032 \pm 0.0002$		$0.0032 \pm 0.0001$		$0.0069 \pm 0.0001$	
45	$0.0015 \pm 0.0001$		$0.0031 \pm 0.0001$		$0.0031 \pm 0.0001$		$0.0059 \pm 0.0001$	
50	$0.0022 \pm 0.0001$		$0.0025 \pm 0.0001$		$0.0025 \pm 0.0001$		$0.0041 \pm 0.0001$	
60	$0.0024 \pm 0.0001$		$0.0018 \pm 0.0001$		$0.0018 \pm 0.0001$		$0.0025 \pm 0.0001$	
70	$0.0017 \pm 0.0001$		$0.0008 \pm 0.0001$		$0.0009 \pm 0.0001$		$0.0015 \pm 0.0001$	
80	$0.0011 \pm 0.0001$							

Table S 3 Time after which  $I/(2\tau)$  of the echo decays of **1H** and **1D** 1mM in **solH** and **solD** at 1258 mT, 35 GHz and different temperatures drop below 10 % of their initial value.

<b>T / K</b>	<b>1D/solD</b>	<b>1H/solD</b>	<b>1D/solH</b>	<b>1H/solH</b>
	$T_{m,10\%} / \mu\text{s}$	$T_{m,10\%} / \mu\text{s}$	$T_{m,10\%} / \mu\text{s}$	$T_{m,10\%} / \mu\text{s}$
7	12.56	16.96	5.832	5.6
10	10.056	11.83	5.128	5.356
15	7.84	9.1	5.208	5.224
20	6.65	7.39	4.784	4.508
25	4.768	5.89	4.36	4.268
30	4.256	4.8	4.1	4.076
35	3.596	3.904	3.656	3.812
40	3.037	3.54	3.548	3.496
45	2.892	3.01	3.018	3.132
50	2.656	2.69	2.432	3.008
60	1.948	2.33	0.73	2.46
70	0.684	2.3	0.412	0.72
80	0.686	1.84		

## II. Detailed derivation of $\Lambda$ tensor

In case of the lighter transition metal ions, magnetic properties are mainly dominated by the spin momentum due to the quenching of angular momentum. However, in the most cases there is still some residual angular momentum left which can be described by second order perturbation using a crystal field basis. The properties of interest can then be calculated by evaluating the  $\Lambda$ -tensor,<sup>2</sup> which connects the crystal field states with the same multiplicity via the angular momentum operator  $\hat{L}$ :

$$\Lambda_{ab} = \sum_{k \neq 0} \frac{\langle 0 | \hat{L}_a | k \rangle \langle k | \hat{L}_b | 0 \rangle}{E_k - E_0}$$

For example, the ZFS parameters  $D$  and  $E$  can be calculated from the  $\Lambda$ -tensor:

$$D = -\frac{1}{2}\zeta^2(2\Lambda_{zz} - \Lambda_{xx} - \Lambda_{yy})$$

$$E = -\frac{1}{2}\zeta^2(\Lambda_{xx} - \Lambda_{yy})$$

We calculate the  $\Lambda$ -tensor for **1** by evaluating the matrix elements  $\langle 0 | \hat{L}_a | k \rangle$  in octahedral symmetry  $O$  for a  $d^3$  electron configuration and account for the real symmetry  $D_2$  of the molecule by applying the chain of groups  $O \supset D_4 \supset D_2$ . In octahedral symmetry, the ground state of our system transform as  $A_2$  while the excited states transform either as  $E$ ,  $T_1$  or  $T_2$ . As the angular momentum operator transform as  $T_1$  and states with different spin-multiplicity are orthogonal only the  $^4T_2$  excited state has to be taken into account. Furthermore, only the diagonal elements of the  $\Lambda$ -tensor are non-zero. The remaining matrix elements  $\langle ^4A_2 | \hat{L}_a | ^4T_2 \rangle^0 \supset D_4 \supset D_2$  can be decomposed into a reduced matrix element  $\langle ^4A_2 | \hat{L}_a | ^4T_2 \rangle^0$ , a 2jm and a 3jm using the Wigner-Eckhart theorem (see Table S4 for the irrep branching table):

$$\langle ^4A_2 | \hat{L}_x | ^4T_2 \rangle^0 \supset D_4 \supset D_2 = \left( \frac{A_2}{B_1} \right) O \cdot \left( \frac{B_1}{A_1} \right) D_4 \cdot \left( \begin{matrix} A_2 & T_1 & T_2 \\ B_1 & E & E \end{matrix} \right) D_4 \cdot \left( \begin{matrix} B_1 & E & E \\ A_1 & B_3 & B_3 \end{matrix} \right) D_2 \cdot \langle ^4A_2 | | L^{T_1} | | ^4T_2 \rangle^0$$

$$\langle ^4A_2 | \hat{L}_y | ^4T_2 \rangle^0 \supset D_4 \supset D_2 = \left( \frac{A_2}{B_1} \right) O \cdot \left( \frac{B_1}{A_1} \right) D_4 \cdot \left( \begin{matrix} A_2 & T_1 & T_2 \\ B_1 & E & E \end{matrix} \right) D_4 \cdot \left( \begin{matrix} B_1 & E & E \\ A_1 & B_2 & B_2 \end{matrix} \right) D_2 \cdot \langle ^4A_2 | | L^{T_1} | | ^4T_2 \rangle^0$$

$$\langle ^4A_2 | \hat{L}_z | ^4T_2 \rangle^0 \supset D_4 \supset D_2 = \left( \frac{A_2}{B_1} \right) O \cdot \left( \frac{B_1}{A_1} \right) D_4 \cdot \left( \begin{matrix} A_2 & T_1 & T_2 \\ B_1 & E & E \end{matrix} \right) D_4 \cdot \left( \begin{matrix} B_1 & E & E \\ A_1 & B_1 & B_1 \end{matrix} \right) D_2 \cdot \langle ^4A_2 | | L^{T_1} | | ^4T_2 \rangle^0$$

$$\langle ^4T_2 | \hat{L}_x | ^4A_2 \rangle^0 \supset D_4 \supset D_2 = \left( \frac{T_2}{E} \right) O \cdot \left( \frac{E}{B_3} \right) D_4 \cdot \left( \begin{matrix} T_2 & T_1 & A_2 \\ E & E & B_1 \end{matrix} \right) D_4 \cdot \left( \begin{matrix} E & E & B_1 \\ B_3 & B_3 & A_1 \end{matrix} \right) D_2 \cdot \langle ^4T_2 | | L^{T_1} | | ^4A_2 \rangle^0$$

$$\langle ^4T_2 | \hat{L}_y | ^4A_2 \rangle^0 \supset D_4 \supset D_2 = \left( \frac{T_2}{E} \right) O \cdot \left( \frac{E}{B_2} \right) D_4 \cdot \left( \begin{matrix} T_2 & T_1 & A_2 \\ E & E & B_1 \end{matrix} \right) D_4 \cdot \left( \begin{matrix} E & E & B_1 \\ B_2 & B_2 & A_1 \end{matrix} \right) D_2 \cdot \langle ^4T_2 | | L^{T_1} | | ^4A_2 \rangle^0$$

$$\langle ^4T_2 | \hat{L}_z | ^4A_2 \rangle^0 \supset D_4 \supset D_2 = \left( \frac{T_2}{E} \right) O \cdot \left( \frac{E}{B_1} \right) D_4 \cdot \left( \begin{matrix} T_2 & T_1 & A_2 \\ E & E & B_1 \end{matrix} \right) D_4 \cdot \left( \begin{matrix} E & E & B_1 \\ B_1 & B_1 & A_1 \end{matrix} \right) D_2 \cdot \langle ^4T_2 | | L^{T_1} | | ^4A_2 \rangle^0$$

The reduced multielectron matrix element  $\langle ^4T_2 | | L^{T_1} | | ^4A_2 \rangle^0$  can be related to the reduced single electron matrix element  $\langle t_2 | | l^{T_1} | | e \rangle^0$  using the concept of fractional coefficients described in Piepho and Schatz.<sup>3</sup> The reduced matrix element  $\langle t_2 | | l^{T_1} | | e \rangle^0$  can be directly calculated by symmetry reduction from  $SO_3$ :

$$\langle ^4A_2 | | L^{T_1} | | ^4T_2 \rangle^0 = \langle ^4T_2 | | L^{T_1} | | ^4A_2 \rangle^0 = \langle t_2 | | l^{T_1} | | e \rangle^0 = \begin{pmatrix} 2 & 1_1 & 2 \\ T_2 & T_1 & E \end{pmatrix} SO_3 \sqrt{l(l+1)(2l+1)} = \left( -\frac{\sqrt{2}}{\sqrt{5}} \right) \sqrt{30} = -2\sqrt{3}$$

The remaining 2jm and 3jm factors can be looked up in the tables of Butler,<sup>4</sup> for example:

$$\left( \frac{A_2}{B_1} \right) O \cdot \left( \frac{B_1}{A_1} \right) D_4 \cdot \left( \begin{matrix} A_2 & T_1 & T_2 \\ B_1 & E & E \end{matrix} \right) D_4 \cdot \left( \begin{matrix} B_1 & E & E \\ A_1 & B_3 & B_3 \end{matrix} \right) D_2 = \begin{pmatrix} 0 \\ \frac{1}{2} \end{pmatrix} O \cdot \begin{pmatrix} 2 \\ 0 \end{pmatrix} D_4 \cdot \begin{pmatrix} 0 & 1 & 1 \\ 2 & 1 & 1 \end{pmatrix} D_2 \cdot \begin{pmatrix} 2 & 1 & 1 \\ 0 & 1 & 1 \end{pmatrix} D_4 = 1 \cdot 1 \cdot \frac{\sqrt{2}}{\sqrt{3}} \cdot \frac{-1}{\sqrt{2}}$$

Finally, we arrive at:

$$\langle {}^4A_2 | \hat{L}_x | {}^4T_2 \rangle^{O \supset D_4 \supset D_2} = \langle {}^4T_2 | \hat{L}_x | {}^4A_2 \rangle^{O \supset D_4 \supset D_2} = +_2$$

$$\langle {}^4A_2 | \hat{L}_y | {}^4T_2 \rangle^{O \supset D_4 \supset D_2} = \langle {}^4T_2 | \hat{L}_y | {}^4A_2 \rangle^{O \supset D_4 \supset D_2} = -_2$$

$$\langle {}^4A_2 | \hat{L}_y | {}^4T_2 \rangle^{O \supset D_4 \supset D_2} = \langle {}^4T_2 | \hat{L}_y | {}^4A_2 \rangle^{O \supset D_4 \supset D_2} = +_2$$

The elements of the  $\Lambda$ -tensor are then:

$$\Lambda_{xx} = \frac{\langle {}^4A_2 | \hat{L}_x | {}^4T_2 \rangle^{O \supset D_4 \supset D_2} \langle {}^4T_2 | \hat{L}_x | {}^4A_2 \rangle^{O \supset D_4 \supset D_2}}{E_1 - E_0} = \frac{4}{E_1}$$

$$\Lambda_{yy} = \frac{\langle {}^4A_2 | \hat{L}_x | {}^4T_2 \rangle^{O \supset D_4 \supset D_2} \langle {}^4T_2 | \hat{L}_x | {}^4A_2 \rangle^{O \supset D_4 \supset D_2}}{E_2 - E_0} = \frac{4}{E_2}$$

$$\Lambda_{zz} = \frac{\langle {}^4A_2 | \hat{L}_x | {}^4T_2 \rangle^{O \supset D_4 \supset D_2} \langle {}^4T_2 | \hat{L}_x | {}^4A_2 \rangle^{O \supset D_4 \supset D_2}}{E_3 - E_0} = \frac{4}{E_3}$$

Table S 4 Branching table for the important irreducible representations for the chain  $O \supset D_4 \supset D_2$ . The symbol in round brackets corresponds to the Butler notation

$O$	$D_4$	$D_2$
$A_2(0)$	$B_1(2)$	$A_1(0)$
$T_1(1)$	$A_2(0) + E(1)$	$B_1(0) + B_2(1) + B_3(1)$
$T_2(1)$	$B_2(2) + E(1)$	$B_1(0) + B_2(1) + B_3(1)$

## References

1. C. Wang, S. Otto, M. Dorn, E. Kreidt, J. Lebon, L. Srsan, P. Di Martino-Fumo, M. Gerhards, U. Resch-Genger, M. Seitz and K. Heinze, *Angew. Chem. Int. Ed.*, 2018, **57**, 1112-1116.
2. R. Boča, *Coord. Chem. Rev.*, 2004, **248**, 757-815.
3. S. B. Piepho and P. N. Schatz, *Group Theory in Spectroscopy with Applications to Magnetic Circular Dichroism*, John Wiley & Sons, New York, 1983.
4. P. H. Butler, *Point Group Symmetry Applications: Methods and Tables*, Plenum Press, New York, 1981.